LETTER Communicated by Markus Diesmann

Synchrony-Induced Switching Behavior of Spike Pattern Attractors Created by Spike-Timing-Dependent Plasticity

Takaaki Aoki
aoki@acs.i.kyoto-u.ac.jp
Graduate School of Informatics, Kyoto University, Kyoto 606-8501, Japan, and CREST, JST, Kyoto 606-8501, Japan

Toshio Aoyagi
aoyagi@i.kyoto-u.ac.jp
Graduate School of Informatics, Kyoto University, Kyoto 606-8501, Japan

Although context-dependent spike synchronization among populations of neurons has been experimentally observed, its functional role remains controversial. In this modeling study, we demonstrate that in a network of spiking neurons organized according to spike-timing-dependent plasticity, an increase in the degree of synchrony of a uniform input can cause transitions between memorized activity patterns in the order presented during learning. Furthermore, context-dependent transitions from a single pattern to multiple patterns can be induced under appropriate learning conditions. These findings suggest one possible functional role of neuronal synchrony in controlling the flow of information by altering the dynamics of the network.

1 Introduction

Although synchronous activity associated with behavior and cognition has been observed in many neuronal systems (Gray, König, Engel, & Singer, 1989; Riehle, Grün, Diesmann, & Aertsen, 1997; Fries, Reynolds, Rorie, & Desimone, 2001), its functional role remains unclear (Engel, Fries, & Singer, 2001; Salinas & Sejnowski, 2001; Shadlen & Movshon, 1999; Ermentrout & Kleinfeld, 2001). It is reasonable to assume that such generated synchronous spikes drive certain cortical networks as input signals and thereby affect their functions (Brody & Hopfield, 2003; Diesmann, Gewaltig, & Aertsen, 1999). Another related phenomenon is spike-timing-dependent plasticity (STDP) (Bi & Poo, 1998; Zhang, Tao, Holt, Harris, & Poo, 1998; Debanne, Gahwiler, & Thompson, 1998; Markram, Lübke, Frotscher, & Sakmann, 1997; Song, Miller, & Abbott, 2000; Rubin, Lee, & Sompolinsky, 2001), which allows cortical networks to learn the causality of experienced events through the coding of the temporal structures of neuronal activity. Considering that both phenomena affect the functioning of cortical neurons, it is

Neural Computation **19, 2720–2738** (2007)

natural to ask what effect synchronous inputs have on a neural network organized under STDP learning. For this purpose, let us consider the specific situation in which a model network of spiking neurons, whose synaptic connections are modified through STDP, receives an activity pattern as an external stimulus as a result of the experiencing of some external events. In general, these activity patterns possess some systematic temporal structure reflecting the causality of these external events (Hebb, 1949; Dan & Poo, 2004; Izhikevich, 2006).

In this study, we demonstrate that a network organized under STDP not only is capable of memorizing the activity patterns of the external stimulus, but also exhibits a systematic transition behavior among the memorized patterns in response to uniform external synchronized spikes. First, in section 2, we describe the structure of the network model and the learning process of STDP. Next, we investigate the behavior of the network organized under STDP, for the case of asynchronous (see section 3.1) and transient synchronized spike inputs (see section 3.2). From these results, to understand the essential mechanism of switching behavior of the network, in section 3.3 we develop a stability analysis of the memorized pattern in a simplified version of the network model. In section 3.4, we also demonstrate that a context-dependent switching behavior can be achieved under some appropriate learning conditions. Finally, in section 4, we discuss the mechanism of the synchrony-induced switching behavior of the network from the point of view of dynamical systems. In relation to recent experimental findings, we discuss the putative functional rules of neuronal synchrony.

2 Model

Figure 1A presents a schematic illustration of the model network we consider, in which leaky integrate-and-fire neurons are recurrently connected by excitatory synapses whose coupling strengths are modified according to the STDP rule (Song et al., 2000; van Rossum, Bi, & Turrigiano, 2000; Cateau & Fukai, 2003). Thus, if a presynaptic spike and a postsynaptic spike occur at times t_{pre} and t_{post}, the peak synaptic conductance g is modified by the addition of the value of the STDP window function $F(t_{\mathrm{pre}} - t_{\mathrm{post}})$, as shown in Figure 1B. The synaptic conductance g is restricted to lie within the range 0 to $g^{\mathrm{E}}_{\mathrm{max}}$. To enforce this restriction, if the STDP rule causes g to take a value outside this range, it is reset to the appropriate limiting value. In addition, a globally uniform inhibition without modification of learning is included in an all-to-all manner (see appendix A for a full description of the simulation).

We employ two types of controllable external inputs. One is a stimulus input, in which an initial stimulus pattern and a training stimulus pattern are presented during a trial and a learning session, respectively. For learning, we use a simple training stimulus pattern, as depicted in Figure 1C. This pattern is divided into three parts consisting of firing patterns, referred

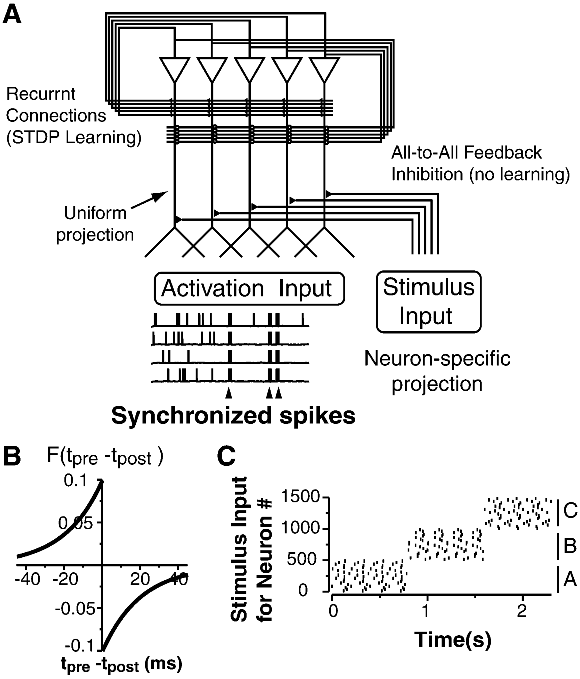

Figure 1: (A) Schematic diagram depicting the structure of the network model with spike-timing-dependent plasticity (STDP). Each leaky integrate-and-fire neuron receives two external inputs. One is a stimulus input, which is a neuron-specific current used to set a given firing pattern in the network for the learning and initial stimulus. The other is an activation input, which projects to all neurons uniformly. For the activation input, there are two modes: asynchronous and synchronous. Within the network, each neuron is connected reciprocally by an excitatory synaptic coupling, whose strength is modified according to the STDP rule. In addition, all-to-all uniformly inhibitory connections are included. (B) The STDP window function. (C) The activity pattern presented by the stimulus input during learning. Each dot represents a spike presented in the corresponding stimulus input. This whole pattern consists of three basic firing patterns in the fixed order A,B,C,A,B,C $\cdots$.

to as A, B, and C, in which each is composed of a particular set of active neurons. These neurons that are active for a given pattern fire periodically, and in each pattern, there are certain fixed phase relationships among the active neurons. During learning, these three patterns are presented as the stimulus input (see Figure 1A) in the fixed order (A,B,C,A,B,C $\cdots$). This can be regarded as representing a certain external sequence of events that the network is to learn—in other words, the causality of certain external events.

The other type of controllable input is an activation input, which projects to all neurons uniformly. This input is introduced to examine the effect of synchrony on the neuronal dynamics. This uniform background input serves to activate the entire network and allow each neuron to be in a firing state under suitable conditions. There are two modes of neuronal activity for the activation input: asynchronous and synchronous modes. In the asynchronous mode, spike trains are randomly generated by a Poisson process. During learning, the activation input is always in the asynchronous mode. In the synchronous mode, some of the neurons fire synchronously, while the other neurons remain in the asynchronous firing state. The fraction of neurons firing synchronously represents the degree of synchrony. To remove the influence of firing-rate modulation, in both modes, the average firing-rate is set to the same constant value, 25 Hz.

3 Results

3.1 Associative Memory Behavior. The main question of interest in this study is the following: After the STDP learning process described above has been completed, what activity pattern does the resultant network exhibit? To answer this question, we first examine the case in which the activation input is set in the asynchronous mode, with the level of the total current such that the neurons are in an active state in response to an appropriate stimulus input and maintain an active state through recurrent excitatory synapses organized under the STDP. In the following simulations, we use the condition that the synaptic weights are fixed after learning. This condition is reasonable under a situation in which the dynamics of the synaptic modification is much slower than that of the spiking activity.

For our model under these conditions, Figure 2A illustrates some typical activity patterns displayed by the network (top), the stimulus input (middle), and the activation input (bottom) as raster plots. In each case, a stimulus input that is close to one of the learned patterns is applied for only a brief initial time interval. Apparently, in the situation considered, the activity pattern rapidly converges to the closest learned pattern. Without an input stimulus, this recalled activity pattern is sustained by the excitatory synaptic connections organized through the learning process and suppresses the other memorized patterns with all-to-all inhibitory connections. Therefore, if the wrong neurons fire accidentally, the network activity is corrected and maintained in a robust manner. Such behavior is of the same type as that typically seen in systems exhibiting associative memory dynamics, like the Hopfield model (Hopfield, 1982), except that these retrieval dynamics contain not only information regarding the firing rate but also that regarding the temporal structure of each learned pattern in the present case.

3.2 Synchrony-Induced Switching Behavior. The situation described above is that in which the system recalls one of the three learned patterns and remains in the corresponding state indefinitely. However, in the

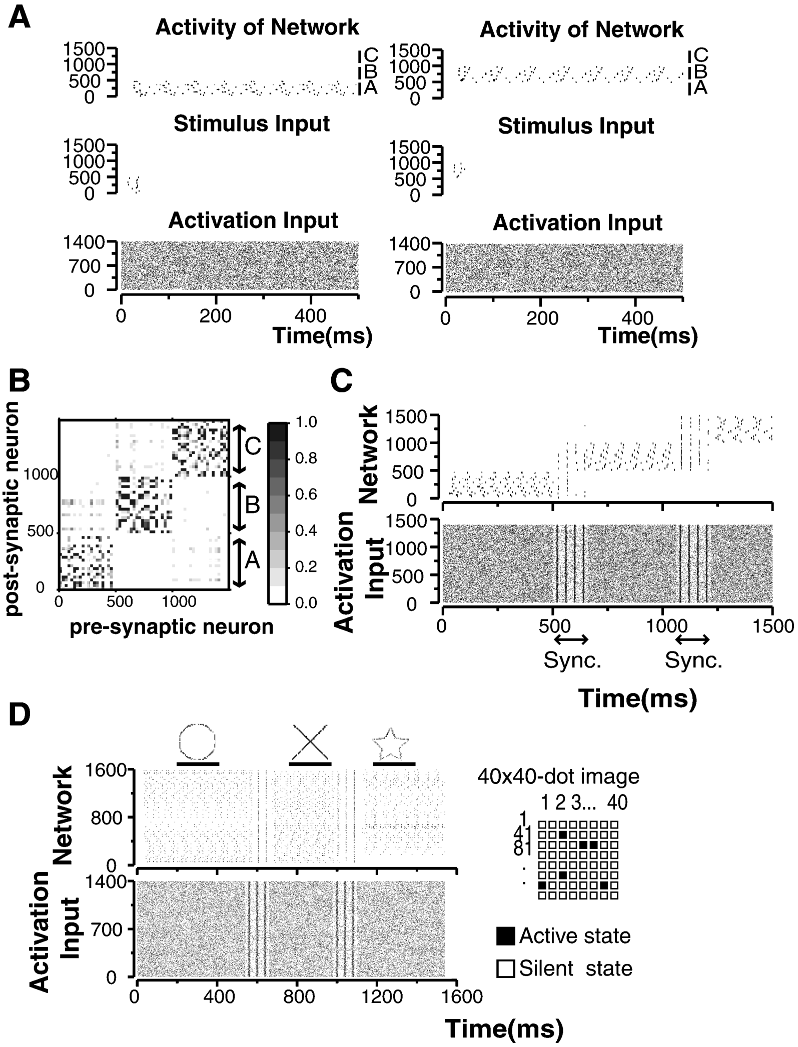
A
Activity of Network
Stimulus Input
Activation Input
1500
1000
500
0
1400
700
C
B
A
0
200
400
Time(ms)
B
post-synaptic neuron
pre-synaptic neuron
1000
500
0
1.0
0.8
0.6
0.4
0.2
0.0
C
Network
Activation Input
1500
1000
500
0
1500
Sync.
Sync.
Time(ms)
D
Network
Activation Input
1600
800
0
1400
700
400
800
1200
1600
Time(ms)
40x40-dot image
1 2 3... 40
1
41
81
Active state
Silent state

learning process, the network learned these three patterns not independently but in the particular order depicted in Figure 1C. This large-scale structure can be interpreted as reflecting the causality of some sequence of external events. Thus, because these transitions themselves are included in the training pattern, they too are encoded in the synaptic matrix (see Figure 2B). However, because during the learning process, the individual patterns A, B, and C are presented many times in succession, while the transitions between these patterns appear much less often, the network has much less experience with these transitions. Hence, the network does not learn these transitions as well as the individual patterns, and therefore the synaptic coupling corresponding to the transitions among patterns is relatively weak. In fact, we can see clearly that three diagonal blocks of major synaptic connections, which are formed by the three basic stimulus patterns (A,B,C), enable the network to retrieve each pattern in an associative manner. In addition, there are three off-diagonal blocks of weak synaptic connections arising from the less frequent transitions among the stimulus patterns as shown in Figure 1C. Because the synaptic connections for transitions are relatively weak, under ordinary conditions, each individual pattern is sufficiently stable that no transition among patterns occurs.

Is there any situation in which these weak synapses arising through STDP from the pattern transitions presented in the learning process yield a substantial effect on the dynamics of the network? Interestingly, Figure 2C demonstrates that a brief period of synchrony in the uniform activation input can enhance this weak effect embedded in the synaptic matrix and thereby cause a transition from the one pattern to another. Let us describe the process depicted in that figure. First, the network exhibits pattern A, which is stable when the activation input is in the asynchronous mode. Thus, in this

---

Figure 2: Typical effect of a uniformly synchronized spike input on the network of spiking neurons organized under the STDP learning rule. (A) Typical activity patterns (top raster plots) in the case that the activation input is in the asynchronous mode (bottom raster plots). In response to the brief presentation of the initial firing pattern of the stimulus input (middle raster plots), the network rapidly converges to the learned pattern that is most similar to this stimulus input. (B) Gray-scale plot of the normalized strengths of excitatory synapses between neurons after the STDP learning. (C) Synchrony-induced switching behavior of the network realized through the STDP learning rule. The situation here is the same as that depicted in Figure 2A, except that in this case, the mode in the activation input temporally changes from asynchrony to synchrony for the time interval indicated by the double-arrowed lines. In response to this brief synchronous activation input, the activity pattern becomes unstable and, consequently, a transition to the next pattern occurs. (D) The same kind of synchrony-induced switching behavior also occurs in the case of more general patterns.

case, the network exhibits ordinary associative memory. However, when the activation input is switched for a brief time to the synchronous mode, a transition from the pattern A to the pattern B occurs. Hence, the retrieval of a learned sequence in the presented order can be triggered by globally uniform synchronous inputs. The off-diagonal weak synaptic connections, as shown in Figure 2B, have no effect on the retrieval dynamics under ordinary conditions, as demonstrated in Figure 2A. However, the effect of these weak synapses can be enhanced by synchronous spike inputs, as shown in Figure 2C.

Note that in the situation studied here, the sets of neurons that are active in patterns A, B, and C are mutually exclusive. This is a somewhat severe restriction. However, we have found that the qualitative nature of these results is the same in the more general case that we allow some of the individual neurons to be active in more than one of the patterns, as long as the number of such neurons is not too large. In fact, we can clearly see from Figure 2D that the same synchrony-induced switching behavior occurs in this case. The top graph shows a 40 × 40 dot image, in which the gray level of a dot represents the average firing rate over 200 ms (black underbars). The condition that a relatively small number of neurons are active in multiple patterns is biologically reasonable, because the mean firing rate of memory patterns is usually low in biological systems (a situation referred to as sparse coding) (Willshaw, Buneman, & Longuet-Higgins, 1969). In addition, it is important to note that many types of observed synchronous activity accompanying cognition and behavior (Gray et al., 1989; Riehle et al., 1997; Fries et al., 2001) are transient, and there have been a number of theoretical studies aimed at understanding the related neuronal mechanism (Aoyagi, Takekawa, & Fukai, 2003; Tiesinga & Sejnowski, 2004).

3.3 Stability Analysis of the Retrieval State. Theoretical analysis is helpful to understand the essential mechanism of synchrony-induced switching, but a full analytical treatment of a synaptic matrix organized through STDP is very difficult. For this reason, we instead consider a simplified version of the synaptic matrix, keeping the essential properties of the original one, as given by

$$g_{ij}^{E} = \frac{g_{\max}^{E}}{N^{\mathrm{P}}}\left[\Theta\left(\sum_{\mu=1}^{\mathrm{P}} \zeta_i^{\mu}\zeta_j^{\mu}\right) + \epsilon\Theta\left(\sum_{\mu=1}^{\mathrm{P}-1} \zeta_i^{\mu+1}\zeta_j^{\mu}\right)\right],$$

$$\Theta(x) = \begin{cases} 1 & (x \geq 0) \\ 0 & (x < 0) \end{cases}, \tag{3.1}$$

where P is the total number of the stored patterns, and ζ_i^{μ} represents the state in the ith neuron in the μth pattern and takes only two values: 1 (firing) and 0 (quiescent). $N^{\mathrm{P}}(=< \sum_i \zeta_i^{\mu} >_{\mu})$ is the averaged number of active neurons

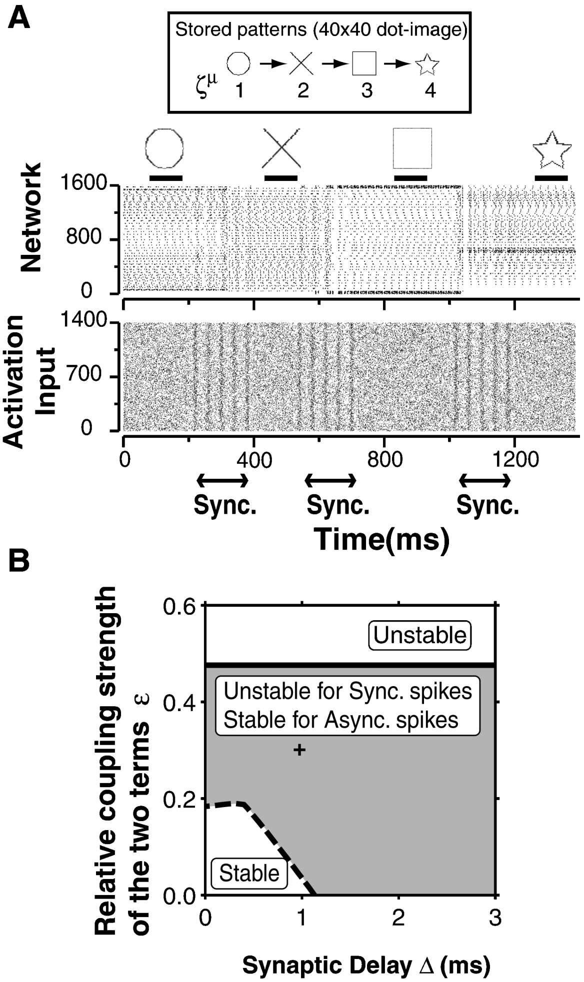

Figure 3: (A) The same synchrony-induced switching behavior can be observed in a simplified version of synapses matrix described in equation 3.1. ($\epsilon = 0.3$) (B) Using this simplified model, we theoretically obtained the two-parameter phase diagram, showing the dependence of the stability of the learned pattern on the synaptic delay Δ and the relative coupling strength ϵ of the two terms. The present state, one of the learned patterns, is stable if the point (Δ, ϵ) is located below the solid curve (dashed curve) for the case of the asynchronous (synchronous) mode of the activation input. In the shaded region, the learned pattern becomes unstable in response to the switching of the mode of the activation input from asynchrony to synchrony. This leads finally to a transition to the next pattern. It is thus seen that the transition-inducing effect of the weak synaptic coupling is enhanced by the synchrony. The parameter values used in Figure 3A are indicated by the +.

over all stored patterns. This simplified matrix is constructed by summing two terms with the relative strength ϵ; the first term ensures the stable retrieval of each learned basic pattern (Hopfield, 1982; Willshaw et al., 1969; Gerstner & van Hemmen, 1992), and the second term is a small term ($\epsilon < 1$) whose effect is to cause a transition among learned patterns.

This simplified matrix makes the previous model theoretically tractable, while providing a reasonable approximation of the original model. In Figure 3A, the same type of synchrony-induced switching behavior can be observed in this simplified model. Using this model, we examined the effect of changing the mode of the activation input on the stability of the current retrieval patterns (see appendix B). The result is displayed in Figure 3B. There, the dependence of the stability on the synaptic delay Δ and the relative coupling strength ϵ of the two terms is plotted.

In the shaded region, the current retrieval pattern is maintained for asynchronous mode in activation input, whereas the same pattern is unstable for synchronous mode. In other words, a change in the stability of the retrieval pattern occurs in response to a synchrony-asynchrony switching in the activation input. This stability analysis does not answer what spike pattern the network exhibits after the synchrony-asynchrony switching. However, considering the effect of the small off-diagonal term in the synaptic weight (see Equation 3.1), which tends to cause the transition among the patterns,

Figure 4: (A) Context-dependent switching behavior can be realized by using the appropriate training pattern. The top and bottom raster plots represent the activity patterns in the network and the activation input, respectively. The lengths of the red double-arrowed lines indicate one period of the firing pattern A, while the red vertical lines indicate the onset times of the switching from asynchrony to synchrony in the activation input. It is thus seen how the network can be caused to make a transition from one given pattern to either of the other two patterns by appropriately controlling the onset time of the synchronous mode. (B) Timing-selective connections organized under STDP reflecting the nature of the training data. For pattern A, the neuron that fires at an early phase has a weak off-diagonal connection for a transition to pattern B, whereas the neuron that fires at a later phase has a connection for pattern C. The normalized strengths of excitatory synapses between neurons are plotted with gray scales. (C) Interpretation of the synchrony-induced switching behavior from the point of view of dynamical systems. When the network is activated by a uniformly asynchronous spike input, the system possesses some attractors formed by the STDP learning rule (left). However, a brief, uniformly synchronous input activates the paths between attractors, leading to a transition to the next pattern in the learned order (middle). Furthermore, the system can exhibit context-dependent switching behavior, in which the subsequently appearing pattern can be determined by appropriately choosing the position of the orbit at the onset time of the synchronous pattern, as demonstrated in Figure 4A (right).

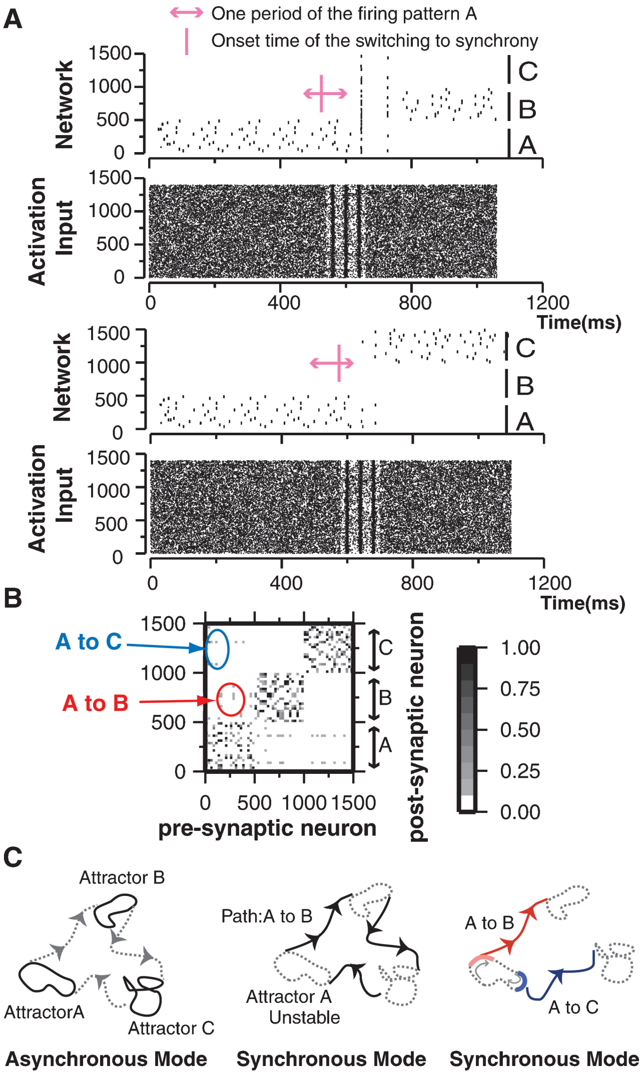
A
One period of the firing pattern A
Onset time of the switching to synchrony
Network
Input Activation
1500
1000
500
0
C
B
A
0
400
800
1200
Time(ms)
B
A to C
A to B
pre-synaptic neuron
post-synaptic neuron
0 500 1000 1500
1.00
0.75
0.50
0.25
0.00
C
Attractor B
AttractorA
Attractor C
Asynchronous Mode
Path:A to B
Attractor A
Unstable
Synchronous Mode
A to B
A to C
Synchronous Mode

it is likely that the state in the network moves near the next learned pattern. Consequently, when the activation input becomes asynchronous again, the network activity converges toward the next learned pattern in an associative manner. For successful transition among the learned patterns, it is required that the length of the period of synchronized spike input is appropriate. In general, the desirable value of this period (100–200 ms in this case) depends on the model parameters. It is found that too short a period cannot trigger the transition to the next pattern, so that the network stays on the same pattern, whereas a period that is too long tends to make the transition uncontrollable. Hence, an appropriate transient synchrony of the activation input is able to activate the effect of the weak coupling and consequently induce a transition from one state to the next in the learned order. In relation to this mechanism, it has been reported that synchrony causes a similar destabilization phenomenon in the case of a winner-take-all competition (Lumer, 2000), and in the case of conventional neural networks, a change in the uniform external field can cause a transition between memorized patterns under suitable conditions (Amit, 1988).

3.4 Context-Dependent Switching Behavior. The synchrony-induced switching mechanism realized in a model with STDP has a greater ability to cause the network to encode the context-dependent association set by the training data. Figure 4A demonstrates that the network is able to make a transition from the pattern A to either pattern B or C, depending on the onset time of the synchronous mode. When the mode of the activation input changes from asynchrony to synchrony early in the period of pattern A, a transition from pattern A to pattern B occurs, whereas when this mode change takes place later in the period, a transition from pattern A to pattern C occurs.

This context-dependent behavior is due to the nature of the training data, in which the transition to pattern B (C) occurs during the first (second) half of a period of firing activity of pattern A. Therefore, the difference in the temporal structure of pattern A at the time of the transition organizes a selective synaptic connection among the neurons: the neurons that fire early in pattern A tend to make excitatory connections to the neurons that fire in pattern B, while the neurons at a later phase form connections to the neurons of pattern C (see Figure 4B). Owing to this selective connection organized under STDP, which patterns (B or C) the network makes a transition to depends on the onset time of the external synchronized spikes, equivalently, the corresponding temporal structure of pattern A. In summary, for the context-dependent switching described to appear, it is necessary that the activity pattern have a temporal structure that varies in time periodically. The temporal firing pattern exhibited by the network depends on the onset time of the synchronous mode. This dependence endows the network with the ability to make a transition from a single pattern to multiple patterns in a context-dependent manner through STDP learning.

4 Conclusion

We have demonstrated that a network organized under STDP is capable of exhibiting synchrony-induced switching behavior, in which a transition from one firing state to another occurs in response to brief, uniform synchronous spike inputs. In the case of uniformly random spike inputs, the firing state converges to the learned pattern that is closest to the external cue stimulus. Then a synchrony-asynchrony transition in the activation input can induce a transition from one pattern to the next in the order that the learned patterns were presented during training. From the perspective of dynamical systems, in the case of the asynchronous mode, the network possesses certain attractors acquired through STDP learning, as shown in Figure 4C (left). The weak synaptic connections formed through the influence of the transitions among training patterns have no effect on the retrieval dynamics in the asynchronous mode. However, when the network is subject to a uniformly synchronous input, the dynamical properties of the network change drastically. This brief synchronous input activates the paths corresponding to the transitions among individual patterns that were weakly encoded in the synaptic matrix during the learning process, leading to a transition between patterns in the order in which they were presented.

This result suggests that synchronous spikes may act as a signal in biological systems, serving to link learned sequences of actions in response to some external stimuli (Riehle et al., 1997; Lee, 2003). Furthermore, the network has the ability to carry out more complicated tasks, as demonstrated in Figure 4A. As shown there, the attractor corresponding to the pattern appearing after the transition can be switched in a context-dependent manner by controlling the position of the orbit on the attractor at the time that the uniform synchronous input is applied (see Figure 4C). Computationally, the mechanism studied here seems to provide a sophisticated method by which a neuronal system can carry out a task in a context-dependent manner. It has been pointed out that although the amount of information encoded by correlated activity may be small, coherent neuronal activity is observed during particular cognitive and behavioral tasks (Salinas & Sejnowski, 2001; Averbeck & Lee, 2004). Our results suggest that one possible functional role of neuronal synchrony is to control the flow of information by changing the nature of the dynamical system constituted by a set of neuronal circuits. We believe that some experimental results can be more clearly reinterpreted using our results.

Appendix A: Detailed Model

A.1. Dynamics. In the network of spiking neurons we employ (see Figure 1A), the dynamics of each neuron are described by a leaky integrate-and-fire model,

$$\tau_{\rm m}\frac{dV_i(t)}{dt} = -(V_i(t) - V_{\rm rest}) + R_{\rm m}\big(I_i^{\rm E}(t) + I^{\rm I}(t)$$
$$+ I^{\rm Act}(t) + I_i^{\rm Stim}(t)\big), \tag{A.1}$$

with $\tau_{\rm m} = 20$ ms, $V_{\rm rest} = -65$ mV, and $R_{\rm m} = 100$ MΩ. Whenever $V_i(t)$ reaches the threshold voltage, $V_{\rm th} = -50$ mV, a spike is generated, and $V_i(t)$ is instantaneously reset to the resting potential, $V_{\rm rest}$. The synaptic currents due to excitatory and inhibitory connections are given by $I_i^{\rm E}(t) = \sum_j^N \sum_n g_{ij}^{\rm E}\alpha(t - t_j^n - \Delta)$ and $I^{\rm I}(t) = -g^{\rm I}\sum_j^N \sum_n \alpha(t - t_j^n - \Delta)$, respectively. Here, each spike-mediated postsynaptic potential is expressed in terms of the α function, which is given by $\alpha(t) = \frac{t}{\tau^2}\exp(\frac{-t}{\tau})$ for $t \geq 0$ and $\alpha(t) = 0$ elsewhere. Here Δ is the synaptic delay, and τ is a time constant. We set $\Delta = 1$ ms and $\tau = 4$ ms/2 ms for excitatory/inhibitory. The values t_j^n ($n = 1, 2, \cdots$) are the spike times of the jth presynaptic neuron. The inhibitory synaptic weight is $g^{\rm I} = 21$ nS uniformly, while the excitatory one, g_{ij}, ranges from 0 to 30 nS ($= g_{\rm max}^{\rm E}$), according to the STDP learning (see Figure 1B). We studied networks consisting of $N = 1500$ (see Figure 2A) and $N = 1600$ neurons (see Figure 2C).

The stimulus current is given by $I_i^{\rm Stim}(t) = g^{\rm Stim}\sum_n \alpha(t - t_{i({\rm Stim})}^n)$, where the quantities $t_{i({\rm Stim})}^n$ ($n = 1, 2, \cdots$) are the times at which the ith neuron receives a spike from the stimulus input. The uniform current from the activation input is given by $I^{\rm Act}(t) = \frac{g^{\rm Act}}{N^{\rm Act}}\sum_k \sum_n \alpha(t - t_{k({\rm Act})}^n)$, where $t_{k({\rm Act})}^n$ ($n = 1, 2, \cdots$) are the spike times of the kth spike train in the activation input. The parameter values $g^{\rm Stim} = 1000$ nS and $g^{\rm Act}/N^{\rm Act} = 5.1$ nS are used. The total number of spike trains in the activation input is 1400. In asynchronous mode, each spike train from the activation input is generated by a Poisson process with frequency 25 Hz. In the synchronous mode, some of the neurons fire synchronously, while the other neurons remain in the asynchronous firing state. The fraction of neurons firing synchronously represents the degree of synchrony (the ratio of synchronized neurons $\rho = 0.6$). In addition, these "synchronized" neurons are not completely synchronized, but exhibit some fluctuation in time, which is generated by a gaussian distribution with $\sigma = 3$ ms. In the case of the simplified model (see Figure 3A), we use the same values for the model parameters, except that we use ratio $\rho = 0.3$ for the degree of synchrony, $g_{\rm max}^{\rm E} = 4.5$ μS for the synaptic weight of excitatory, and $\tau = 4$ ms for the synaptic time constant of both excitatory and inhibitory neurons.

A.2. STDP Learning. For each pair of pre- and postsynaptic spikes, the corresponding synaptic conductance is modified by $g \rightarrow$

$g + F(t_{\mathrm{pre}} - t_{\mathrm{post}})$. The STDP window function $F(t_{\mathrm{pre}} - t_{\mathrm{post}})$ is then given by

$$F(t_{\mathrm{pre}} - t_{\mathrm{post}}) = \begin{cases} A_{+} \exp(\frac{-\|\Delta t\|}{\tau}) & (\Delta t \leq 0) \\ -A_{-} \exp(\frac{-\|\Delta t\|}{\tau}) & (\Delta t > 0) \end{cases}, \tag{A.2}$$

where τ is the time constant of the exponential decay, which determines the effective time range of the STDP window function. The synaptic weights are updated by the STDP update rule every time a postsynaptic neuron receives a spike. When the axonal synaptic delay Δ is taken into account, the effective time difference to be used in the update rule is modified to be $\Delta t = t_{\mathrm{pre}} + \Delta - t_{\mathrm{post}}$. To avoid unlimited synaptic growth, the ratio of the negative and positive area of the STDP window function, A_{-}/A_{+}, must be a sightly larger than 1 (we set $A_{-}/A_{+} = 1.05$) (Song et al., 2000). In addition, the synaptic conductance is restricted to the range 0 to $g^{\mathrm{E}}_{\max}$. We also examine a multiplicative type of STDP rule (Gutig, Aharonov, Rotter, & Sompolinsky, 2003), which is given by

$$F(t_{\mathrm{pre}} - t_{\mathrm{post}}) = \begin{cases} A_{+}(1 - w)^{\mu} \exp(\frac{-\|\Delta t\|}{\tau}) & (\Delta t \leq 0) \\ -A_{-} w^{\mu} \exp(\frac{-\|\Delta t\|}{\tau}) & (\Delta t > 0) \end{cases}, \tag{A.3}$$

where $w = \frac{g}{g^{\mathrm{E}}_{\max}}$ is the normalized synaptic weight and μ is a parameter controlling the weight dependency of synaptic growth. When $\mu = 0$, this STDP rule equals the additive type of STDP rule in equation A.2. In the case of $\mu = 0.05$, 0.2, and 1.0, the obtained synaptic weight matrices are very similar to the synaptic matrix in Figure 2B. We confirmed that the synchrony-induced switching behavior can also be observed in these synaptic matrices (data not shown).

In STDP learning, a stimulus input is used to present some training stimulus patterns. The training stimulus pattern consists of three patterns (A, B, C in Figure 1C), in which the neurons belonging to a pattern fire with a period of 200 ms, keeping certain phase relationships among the firing times of these neurons. In the preliminary learning process, each stimulus pattern is presented for 1200 ms in the fixed order shown in Figure 1C. This order can be regarded as reflecting the causality of experienced external events. It is expected that after this procedure, the network is able to maintain each learned pattern without persistent stimulus input, but further learning is required to facilitate transitions between the learned patterns. For this purpose, in the main learning process, each stimulus pattern is presented for 200 ms in the fixed order A,B,C,A,B,C,A $\cdots$. Between the presentations of each stimulus pattern, there is a quiescent interval period. The duration of each quiescent interval is selected randomly from [100 ms, 300 ms]. The use of various interval times is necessary to ensure that the transition is not associated specifically with a particular interval time, because it is desirable for the network to have the property that the transition can occur at any time within some suitable interval. Typically, this main learning process is repeated several times. In the case depicted in Figure 4A, the learning process is the same, except that the period of each quiescent interval between two stimulus patterns depends on the next pattern (80 ms for A → B, 180 ms for A → C), and the stimulus presentation order is A,B,A,C,A,B,A,C · · ·. This ensures that the transition property depends on the specific timing of the period in activation pattern A. During learning, the activation input is always set in the asynchronous mode.

A.3. Dot Image Plotting of the Firing Pattern of Neurons. In Figures 2D and 3A, describing the numerical simulations, the active firing pattern of the network is a dot image in which neurons are arranged on grid points, and the gray level of the dots indicates the average firing rate over 200 ms (see Figure 2D) and 100 ms (see Figure 3A), normalized with respect to the maximum firing rate.

Appendix B: Stability Analysis in the Retrieval State

We derived the stability condition for the retrieval state in the simplified model with nonoverlapping learned patterns. In particular, we examine the difference of the stability in the two situations that the mode of the activation input is asynchronous and synchronous. Using the rescaled membrane potential $v(t) = V(t) - V_{\mathrm{rest}}$, the dynamics of each neuron can be rewritten by

$$\tau_{\mathrm{m}} \frac{dv_i(t)}{dt} = -v_i(t) + R_{\mathrm{m}} \left(I_i^{\mathrm{E}}(t) + I^{\mathrm{I}}(t) + I^{\mathrm{Act}}(t) \right). \tag{B.1}$$

In the limit of the number of the spike train $N^{\mathrm{Act}} \to \infty$, the synaptic current produced by the activation input can be simplified,

$$I^{\mathrm{Act}}(t) = \begin{cases} \frac{g^{\mathrm{Act}}}{T^{\mathrm{Act}}} \quad \text{(asynchronous)} \\ \frac{(1-\rho)g^{\mathrm{Act}}}{T^{\mathrm{Act}}} + \rho g^{\mathrm{Act}} \sum_n \alpha(t + nT^{\mathrm{Act}}), \\ (n : \text{integer}) \quad \text{(synchronous)} \end{cases} \tag{B.2}$$

where T^{Act} is the period of the synchronized spike in the activation input. In this analysis, the degree of synchrony is controlled by changing the ratio of the synchronized neurons ρ $(0 \le \rho \le 1)$. In other words, ρN^{Act} spike trains are completely synchronized with no jitter, and $(1 - \rho)N^{\mathrm{Act}}$ spike trains are generated randomly with Poisson process. The synaptic currents of the recurrent connections $I_i^{\mathrm{E}}(t)$, $I^{\mathrm{I}}(t)$ are given by

$$I_i^{\mathrm{E}}(t)=\sum_j^N\sum_n g_{ij}^{\mathrm{E}}\alpha(t-\Delta-t_j^n), \qquad I^{\mathrm{I}}(t)=-g^{\mathrm{I}}\sum_j^N\sum_n \alpha(t-\Delta-t_j^n),$$

$$g^{\mathrm{I}}=\frac{g_c^{\mathrm{I}}}{N} \tag{B.3}$$

$$g_{ij}^E=\frac{g_{\mathrm{max}}^E}{N^{\mathrm{P}}}\left[\Theta\left(\sum_{\mu=1}^{\mathrm{P}}\zeta_i^\mu\zeta_j^\mu\right)+\epsilon\Theta\left(\sum_{\mu=1}^{\mathrm{P}-1}\zeta_i^{\mu+1}\zeta_j^\mu\right)\right],$$

$$\Theta(x)=\begin{cases}1 & (x\geq 0)\\ 0 & (x<0)\end{cases}, \tag{B.4}$$

where $N^{\mathrm{P}}(=<\sum_i\zeta_i^\mu>_\mu)$ is the averaged number of active neurons over all stored patterns. To evaluate these currents, we have to determine the spike time t_j^n for the active neurons. From typical results of our numerical simulation for the asynchronous mode, these active neurons tend to fire in a certain period T with independently random phases. In contrast, in the synchronous mode, the neurons tend to fire with a fixed delay θ to the incoming synchronized spikes. Assuming the above conditions, we can simplify the currents $I_i^{\mathrm{E}}(t)$ and $I^{\mathrm{I}}(t)$ in the limit of $N^{\mathrm{P}}, N\rightarrow\infty$. On substituting these equations into equation B.1, we obtain

$$\tau_{\mathrm{m}}\frac{dv_i(t)}{dt}=\begin{cases}-v_i(t)+R_{\mathrm{m}}\left(\dfrac{(g_{\mathrm{max}}^{\mathrm{E}}-g_c^{\mathrm{I}})}{T}+I^{\mathrm{Act}}(t)\right) & \text{(asynchronous)}\\ -v_i(t)+R_{\mathrm{m}}\big((g_{\mathrm{max}}^{\mathrm{E}}-g_c^{\mathrm{I}})\sum_n\alpha(t-\Delta-T^{\mathrm{Act}}(n+\theta)) & \\ \quad +I^{\mathrm{Act}}(t)\big) \quad \text{(synchronous)} & \end{cases}, \tag{B.5}$$

where T and θ are unknown parameters to be solved later. In order to determine these unknown parameters, by integrating equation B.5 over a spike period of the active neurons, we can derive a self-consistent equation,

$$\begin{cases}T=\tau_{\mathrm{m}}\log\left(\dfrac{g^{\mathrm{Act}}/T_{\mathrm{Act}}+\left(g_{\mathrm{max}}^{\mathrm{E}}-g_c^{\mathrm{I}}\right)/T}{g^{\mathrm{Act}}/T_{\mathrm{Act}}+\left(g_{\mathrm{max}}^{\mathrm{E}}-g_c^{\mathrm{I}}\right)/T-\frac{V_{\mathrm{th}}-V_{\mathrm{rest}}}{R_{\mathrm{m}}}}\right) \quad \text{(asynchronous)}\\ \dfrac{V_{\mathrm{th}}-V_{\mathrm{rest}}}{R_{\mathrm{m}}}\tau_{\mathrm{m}}=\dfrac{(1-\rho)\tau_{\mathrm{m}}(1-e^{T_{\mathrm{Act}}/\tau_{\mathrm{m}}})g^{\mathrm{Act}}}{T_{\mathrm{Act}}} \\ \qquad +(g_{\mathrm{max}}^{\mathrm{E}}-g_c^{\mathrm{I}})K_{T_{\mathrm{Act}}}(-\Delta)+\rho g^{\mathrm{Act}}K_{T_{\mathrm{Act}}}(\theta T_{\mathrm{Act}}) \quad \text{(synchronous)}\end{cases}, \tag{B.6}$$

$$K_T(s) \equiv e^{-T/\tau_{\mathrm{m}}} \int_0^T e^{s/\tau_{\mathrm{m}}} \sum_n \alpha(u + s + nT) du. \tag{B.7}$$

If the self-consistent values of T and θ are within physically meaningful ranges, we can determine a solution of equation B.6 for active neurons.

In addition to the above analysis for the active neurons, one more necessary condition for inactive neurons is required: the inactive neuron must not fire when synaptic current is received from the active neurons. In fact, we numerically found that irregular firing in the inactive neuron could perturb the current retrieval state and cause instability. Therefore, we need to check that the membrane potential of the inactive neurons stays below the threshold voltage of the neuronal spike. Among the inactive neurons, the neurons that should fire in the next learned pattern have a higher membrane potential, owing to the excitatory connections from the current active neurons, that is, the second term in equation B.4. From this consideration, it is sufficient that we check only the membrane potential of these neurons, which is described by

$$\tau_{\mathrm{m}} \frac{dv_i(t)}{dt} = \begin{cases} -v_i(t) + R_{\mathrm{m}} \left(\dfrac{(\epsilon g^{\mathrm{E}}_{\mathrm{max}} - g^{\mathrm{I}}_c)}{T} + I^{\mathrm{Act}}(t) \right) & \text{(asynchronous)} \\ -v_i(t) + R_{\mathrm{m}} \big((\epsilon g^{\mathrm{E}}_{\mathrm{max}} - g^{\mathrm{I}}_c) \sum_n \alpha(t - \Delta - T^{\mathrm{Act}}(n + \theta)) & \\ \quad + I^{\mathrm{Act}}(t) \big) \quad \text{(synchronous)} & \end{cases} . \tag{B.8}$$

To evaluate the maximum of the membrane potential, it is useful to derive a return map of $v_i(t)$, which is calculated by integrating over one spike period of the active neurons. The convergent value of the return map is given by

$$v^{\infty}(t') = \begin{cases} R_{\mathrm{m}} \left(\dfrac{\epsilon g^{\mathrm{E}}_{\mathrm{max}} - g^{\mathrm{I}}_c}{T} + \dfrac{g^{\mathrm{Act}}}{T_{\mathrm{Act}}} \right) \quad \text{(asynchronous)} \\ R_{\mathrm{m}} \dfrac{\dfrac{(1-\rho)(1 - e^{T_{\mathrm{Act}}/\tau_{\mathrm{m}}}) g^{\mathrm{Act}}}{T_{\mathrm{Act}}} + \dfrac{(\epsilon g^{\mathrm{E}}_{\mathrm{max}} - g^{\mathrm{I}}_c)}{\tau_{\mathrm{m}}} K_{T_{\mathrm{Act}}}((t' - \theta) T_{\mathrm{Act}} - \Delta) + \dfrac{\rho g^{\mathrm{Act}}}{\tau_{\mathrm{m}}} K_{T_{\mathrm{Act}}}(\theta T_{\mathrm{Act}})}{1 - e^{-T_{\mathrm{Act}}/\tau_{\mathrm{m}}}} , \\ \quad \text{(synchronous)} \end{cases} \tag{B.9}$$

where t' takes from 0 to 1. Finally, the condition for the membrane potential of the inactive neuron is given by

$$V_{\mathrm{th}} > V_{\mathrm{rest}} + \max_{t' \in [0,1)} v^{\infty}(t'). \tag{B.10}$$

The result of Figure 3B is obtained by calculating equations B.6 and B.10.

Acknowledgments

This work was supported by CREST (Core Research for Evolutional Science and Technology) of Japan Science and Technology Corporation (JST) and by Grant-in-Aid for Scientific Research from the Ministry of Education, Science, Sports, and Culture of Japan: Grant number 18047014; 18019019 and 18300079.

References

Amit, D. J. (1988). Neural networks counting chimes. *Proc. Natl. Acad. Sci. USA, 85*, 2141–2145.

Aoyagi, T., Takekawa, T., & Fukai, T. (2003). Gamma rhythmic bursts: Coherence control in networks of cortical pyramidal neurons. *Neural Comput., 15*, 1035–1061.

Averbeck, B. B., & Lee, D. (2004). Coding and transmission of information by neural ensembles. *Trends in Neurosci., 27*, 225–230.

Bi, G. Q., & Poo, M. M. (1998). Synaptic modifications in cultured hippocampal neurons: Dependence on spike timing, synaptic strength, and postsynaptic cell type. *J. Neurosci., 18*, 10464–10472.

Brody, C. D., & Hopfield, J. J. (2003). Simple networks for spike-timing-based computation, with application to olfactory processing. *Neuron, 37*, 843–852.

Cateau, H., & Fukai, T. (2003). A stochastic method to predict the consequence of arbitrary forms of spike-timing-dependent plasticity. *Neural Comput., 15*, 597–620.

Dan, Y., & Poo, M. M. (2004). Spike timing-dependent plasticity of neural circuits. *Neuron, 44*, 23–30.

Debanne, D., Gahwiler, B. H., & Thompson, S. M. (1998). Long-term synaptic plasticity between pairs of individual CA3 pyramidal cells in rat hippocampal slice cultures. *J. Physiol., 507*, 237–247.

Diesmann, M., Gewaltig, M. O., & Aertsen, A. (1999). Stable propagation of synchronous spiking in cortical neural networks. *Nature, 402*, 529–533.

Engel, A. K., Fries, P., & Singer, W. (2001). Dynamic predictions: Oscillations and synchrony in top-down processing. *Nat. Rev. Neurosci., 2*, 704–716.

Ermentrout, G. B., & Kleinfeld, D. (2001). Traveling electrical waves in cortex: Insights from phase dynamics and speculation on a computational role. *Neuron, 29*, 33–44.

Fries, P., Reynolds, J. H., Rorie, A. E., & Desimone, R. (2001). Modulation of oscillatory neuronal synchronization by selective visual attention. *Science, 291*, 1560–1563.

Gerstner, W., & van Hemmen, J. L. (1992). Associative memory in a network of "spiking" neurons. *Network: Comput. Neural Syst., 3*, 139–164.

Gray, C. M., König, P., Engel, A. K., & Singer, W. (1989). Oscillatory responses in cat visual cortex exhibit inter-columnar synchronization which reflects global stimulus properties. *Nature, 338*, 334–337.

Gutig, R., Aharonov, R., Rotter, S., & Sompolinsky, H. (2003). Learning input correlations through nonlinear temporally asymmetric Hebbian plasticity. *J. Neurosci., 23*, 3697–3714.

Hebb, D. O. (1949). *The organization of behavior: A neuropsychological theory.* New York: Wiley.

Hopfield, J. J. (1982). Neural networks and physical systems with emergent collective computational abilities. *Proc. Natl. Acad. Sci. USA, 79*, 2554–2558.

Izhikevich, E. M. (2006). Polychronization: Computation with spikes. *Neural Comput., 18*, 245–282.

Lee, D. (2003). Coherent oscillations in neuronal activity of the supplementary motor area during a visuomotor task. *J. Neurosci., 23*, 6798–6809.

Lumer, E. D. (2000). Effects of spike timing on winner-take-all competition in model cortical circuits. *Neural Comput., 12*, 181–194.

Markram, H., Lübke, J., Frotscher, M., & Sakmann, B. (1997). Regulation of synaptic efficacy by coincidence of postsynaptic APS and EPSPs. *Science, 275*, 213–215.

Riehle, A., Grün, S., Diesmann, M., & Aertsen, A. (1997). Spike synchronization and rate modulation differentially involved in motor cortical function. *Science, 278*, 1950–1953.

Rubin, J., Lee, D. D., & Sompolinsky, H. (2001). Equilibrium properties of temporally asymmetric Hebbian plasticity. *Phys. Rev. Lett., 86*, 364–367.

Salinas, E., & Sejnowski, T. J. (2001). Correlated neuronal activity and the flow of neural information. *Nat. Rev. Neurosci., 2*, 539–550.

Shadlen, M. N., & Movshon, J. A. (1999). Synchrony unbound: A critical evaluation of the temporal binding hypothesis. *Neuron, 24*, 67–77.

Song, S., Miller, K. D., & Abbott, L. F. (2000). Competitive Hebbian learning through spike-timing-dependent synaptic plasticity. *Nat. Neurosci., 3*, 919–926.

Tiesinga, P. H., & Sejnowski, T. J. (2004). Rapid temporal modulation of synchrony by competition in cortical interneuron networks. *Neural Comput., 16*, 251–275.

van Rossum, M. C., Bi, G. Q., & Turrigiano, G. G. (2000). Stable Hebbian learning from spike timing-dependent plasticity. *J. Neurosci., 20*, 8812–8821.

Willshaw, D. J., Buneman, O. P., & Longuet-Higgins, H. C. (1969). Non-holographic associative memory. *Nature, 222*, 960–962.

Zhang, L. I., Tao, H. W., Holt, C. E., Harris, W. A., & Poo, M. (1998). A critical window for cooperation and competition among developing retinotectal synapses. *Nature, 395*, 37–44.

Received April 16, 2006; accepted September 2, 2006.